HHS Public Access

Author manuscript

Nat Neurosci. Author manuscript; available in PMC 2018 January 17.

Published in final edited form as:

Nat Neurosci. 2017 September ; 20(9): 1260–1268. doi:10.1038/nn.4607.

A circuit-based mechanism underlying familiarity signaling and the preference for novelty

Susanna Molas[1], **Rubing Zhao-Shea**[1], **Liwang Liu**[1], **Steven R. DeGroot**[1,2], **Paul D. Gardner**[1], and **Andrew R. Tapper**[1,*]

[1]Brudnick Neuropsychiatric Research Institute, Dept. of Psychiatry, University of Massachusetts Medical School, Worcester, MA, 01604, USA

[2]Graduate Program in Neuroscience, University of Massachusetts Medical School, Worcester, MA, 01604, US

Abstract

Novelty preference (NP) is an evolutionarily conserved, essential survival mechanism often dysregulated in neuropsychiatric disorders. NP is mediated by a motivational dopamine signal that increases in response to novel stimuli thereby driving exploration. However, the mechanism by which once novel stimuli transitions to familiar stimuli is unknown. Here we describe a neuroanatomical substrate for familiarity signaling, the interpeduncular nucleus (IPN) of the midbrain, which is activated as novel stimuli become familiar with multiple exposures. Optogenetic silencing of IPN neurons increases salience of and interaction with familiar stimuli without affecting novelty responses; whereas, photo-activation of the same neurons reduces exploration of novel stimuli mimicking familiarity. Bi-directional control of NP by the IPN depends on familiarity- and novelty-signals arising from excitatory habenula and dopaminergic ventral tegmental area inputs, which activate and reduce IPN activity, respectively. These results demonstrate that familiarity signals through unique IPN circuitry that opposes novelty seeking to control NP.

Introduction

The capacity to detect and react to novel as opposed to familiar stimuli provides an opportunity of adaptation in a rapidly changing environment[1]. Inappropriate response towards novelty is associated with a number of neurodevelopmental and neuropsychiatric disorders including schizophrenia[2], autistic-related behaviors[3], attention deficit hyperactivity disorders, and addiction[4–6]. Although the expression of novelty preference (NP) involves cognitive function and recognition memory[7,8], response to novel events depends on the

*Correspondence to: andrew.tapper@umassmed.edu.

Author Contributions: S.M. and A.R.T. conceived of this study. S.M., R.Z., L.L, S.D., P.D.G. and A.R.T. designed the experiments. S.M., R.Z., L.L, and S.D. performed the experiments. S.M., R.Z., L.L., S.D. and A.R.T. analyzed data. S.M., P.D.G., and A.R.T. wrote the manuscript.

Competing Financial Intersts: The authors declare that they have no competing financial interests.

activation of midbrain reward systems[9], including the dopaminergic (DAergic) neuron-rich substantia nigra (SN) and ventral tegmental area (VTA), which exhibit greater activity when individuals face novel stimuli and lower activity once these stimuli become familiar. This response to novelty is likely correlated with DAergic neuron responses linked to higher novel stimuli saliency as compared to familiar stimuli[10]. However, how a novel stimulus transitions to a familiar stimulus after repeated exposures and how the brain detects familiarity to cease responding is unknown. In addition, whether signaling of novel and familiar stimuli act through distinct neural pathways or share common circuitry has not been explored.

Results

To address the behavioral and neural responses to familiar and novel stimuli, we adapted a paradigm of social interaction using a three-chamber interaction context[11]. In this procedure (Fig. 1a) adult male C57BL/6 mice were tested for sociability towards familiar or novel individuals by receiving the same 4–7-week-old juvenile C57BL/6 male mouse for 3 consecutive days (termed “Familiar-Social”, F-S) or receiving a new stranger individual on the third day (termed “Novel-Social”, N-S). The F-S group exhibited high social investigation rate during the first encounter to a novel social stimulus (N_1) that decreased on days 2 and 3, as the stimulus became familiar (F_1 and F_2, respectively) (Fig. 1b–c). Non-social investigation (of the empty cup) progressively increased from N_1 to F_1 and F_2 (Fig. 1b, d), resulting overall in a reduced social preference ratio across sessions (Fig. 1e). Conversely, the N-S group presented to a novel social stimulus (N_2) on day 3, exhibited rebounded social investigation (Fig. 1b–c) and reduced non-social investigation (Fig. 1b, d), altogether increasing the social preference ratio (Fig. 1e). Both the F-S and N-S groups demonstrated similar total amounts of investigation (Fig. 1f).

To explore the neural circuits underlying the response to novelty and familiarity, we focused on the interpeduncular nucleus (IPN), a brain region medial and ventral to the VTA, but with opposing roles in reward vs. aversion signaling[12]. Recently, IPN activity has been associated with social conflict resolution in zebrafish[13]. However, no studies have addressed the potential role of the IPN in response to social novelty and familiarity in mammals. To map IPN activity during familiar and novel events, we examined Fos immunoreactivity, a marker for neuronal activation[14], 90 min after a social encounter. In control animals that did not experience any social interaction (termed “Non-social”, Non-S), few Fos-positive nuclei were observed in the IPN (Fig. 1g–h). However, the F-S group exhibited an elevated number of Fos-positive nuclei, particularly in the central/ventral portion of the IPN (Fig. 1g–h). In contrast, this neuronal activation was not observed in the N-S group (Fig. 1g–h). Importantly, each juvenile mouse in this task was placed in the same cylinder and compartment within each experiment to avoid effects of novel spatial information, thus, IPN activation solely reflects novel social interaction. These results suggested that the IPN is exclusively activated by an experience-dependent (familiar) social stimulus, but not by social interaction *per se*. We next asked whether activation of the IPN persisted or increased with the degree of familiarity. To this aim, another group of C57BL/6 mice progressively encountered the same individual for 7 consecutive days and we measured the relative IPN activity at different time points (Fig. s1a). As compared to control mice not exposed to a

social stimulus, a first encounter to a novel individual (N_1) did not significantly increase Fos expression in the IPN (Fig. s1b), consistent with the observation that IPN neurons overall were not activated by novel stimuli. A single exposure to the same familiar individual (F_1) was sufficient to significantly raise IPN Fos expression (Fig. s1b). In addition, after repeated presentations to the same individual, IPN neuronal activation progressively increased and reached the highest levels on day 5 (F_4), as demonstrated by an approximately 2.4-fold increase in Fos expression (Fig. s1b).

We also addressed whether changes in IPN activity are associated with general familiar and novel responses using inanimate objects instead of social stimuli. Mice were presented to the same object for 3 consecutive days (termed “Familiar-Object,” F-O), or to a new object on the third day (termed “Novel-Object,” N-O) (Fig. s1c). The F-O group decreased investigation rates from N_1 to F_2, as the object became familiar, whereas the N-O group showed rebounded exploratory behavior to the new item (N_2) (Fig. s1d–e). Interestingly, the F-O group exhibited high number of IPN Fos-positive nuclei that was not seen in the N-O group (Fig. s1f–g).

To define the IPN neuronal population activated by familiar stimuli we used immuno-colocalization analysis of Fos with glutamate acid decarboxylase (GAD2/1), a marker for GABAergic neurons[15]. Double-labeling (Fig. 1i) revealed that ~ 70% (75.19 ± 19.15, n = 3 mice) of the Fos-immunopositive neurons in the F-S group colocalized with GAD2/1 staining, suggesting that the majority of activated neurons in the IPN are inhibitory. We hypothesized that IPN GABAergic neuronal activation may act as a brake for novelty-induced exploratory behavior as novel stimuli become familiar. To test this hypothesis, we selectively targeted IPN GABAergic neurons by injecting a Cre-dependent adeno-associated virus (AAV) encoding halorhodopsin (NpHR3.0) fused to enhanced yellow fluorescent protein (eYFP)[16] into the IPN of mice expressing Cre under the control of the promoter for the gene encoding glutamic acid decarboxylase 2, *GAD2::Cre* mice (*GAD2*^{Cre}::NpHR^{IPN}) (Fig. 2a–b). Numerous eYFP signal-positive (eYFP$^+$) cell bodies in the IPN colocalized with GAD2 staining, verifying the virus is restricted to GABAergic neurons (Fig. 2b). Efficient photo-stimulation-dependent silencing was confirmed in spontaneously active eYFP$^+$-NpHR-expressing current-clamped neurons from the injected animals (Fig. 2c). Importantly, *GAD2*^{Cre}::NpHR^{IPN} photo-stimulation parameters produced robust IPN inhibition without rebound neuronal firing. To assess the requirement of IPN GABAergic activity in familiarity responses, *GAD2*^{Cre}::NpHR^{IPN} mice implanted with an optic fiber in the IPN were presented for 2 consecutive days to the same social stimulus without light delivery, in order to avoid any putative effect on memory acquisition. On the third day, mice were offered the choice between F-S and N-S stimuli whilst half of the group received light illumination (Fig. 2d). Control mice without light exhibited higher investigation towards N-S (Fig. 2e, g) as compared to F-S stimuli (Fig. 2e–f), and a positive NP ratio (Fig. 2h). In contrast, photo-inhibited mice (593 nm, constant light, 20 s ON, 10 s OFF) showed significantly higher F-S investigation compared to controls (light-OFF mice, Fig. 2e–f), mimicking a novelty situation. N-S investigation was not affected by *GAD2*^{Cre}::NpHR^{IPN} photo-inhibition (Fig. 2e, g), confirming that the activity of IPN GABAergic neurons is specific for familiarity signaling. Consequently, the NP ratio was significantly reduced in photo-active *GAD2*^{Cre}::NpHR^{IPN} (Fig. 2h), without interfering with total time of exploratory behavior

(Fig. 2i). Locomotor activity (Fig. s2a) was not significantly affected by *GAD2*^{Cre}::NpHR^{IPN} photo-inhibition. Importantly, *GAD2*^{Cre}::NpHR^{IPN} photo-illumination increased exploration only towards F-S stimuli but not N-S stimuli when mice were exposed to familiar or novel mice once daily during consecutive days (i.e., when mice did not have a choice between exploring novel and familiar stimuli during the same session, Fig. s2b–f). These data suggest that the activity of IPN GABAergic neurons might reversibly control the saliency of familiar vs. novel exploration, rather than memory discrimination. To confirm this idea, we also used a modified version of the conditioned place preference (CPP) paradigm in which mice associated one of two compartments with either F-S or N-S presentations (Fig. s3a). Control mice without light developed a CPP for the N-S compartment (Fig. s3b, d), supporting the notion that interactions with novel stimuli are more rewarding than with familiar ones. In contrast, mice that received photo-inhibition of IPN GABAergic neurons paired with the F-S compartment, preferred the F-S over the N-S compartment (Fig. s3c, d) indicating IPN activation reduces motivation to explore familiar stimuli. Importantly, IPN GABAergic photo-inhibition did not cause significant reward effects during real-time place-preference testing (without social stimuli) (Fig. s3e).

We also tested whether photo-inhibition affected investigation towards inanimate familiar objects (Fig. s4a). *GAD2*^{Cre}::NpHR^{IPN} photo-inhibition increased exploration of familiar but not novel inanimate objects when mice were offered the choice between F-O and N-O stimuli (Fig. s4b–f) or when singly presented with either F-O or N-O stimuli (Fig. s4g–i), suggesting that olfactory cues are not essential for optogenetically-evoked heightened exploration of familiar social stimuli, indicating that IPN activation determines the reduced saliency of familiarity itself.

To test more directly whether familiarity responses could be triggered by optogenetic activation of IPN GABAergic neurons, we expressed Cre-dependent ChR2-eYFP in the IPN of *GAD2::Cre* mice (Fig. 2a)[17]. Light delivery (20 Hz) elicited neuronal firing from ChR2-expressing GAD2 cells with high temporal precision (Fig. 2c) confirming functional expression of ChR2. When offered the choice between N-S and F-S stimuli (Fig. 2d), photo-activation of IPN GABAergic cell bodies (473 nm, 20 Hz, 12 ms pulse for 5 min) significantly decreased N-S investigation (Fig. 2j, l) compared to control mice (light-OFF), mimicking a familiarity response. In contrast, F-S investigation remained unaffected (Fig. 2j–k), thus, significantly decreasing the NP ratio (Fig. 2m) but not total exploratory behavior (Fig. 2n). Similar results were obtained comparing ChR2-expressing mice with non-opsin, eYFP-expressing animals receiving photo-stimulation (Fig. s5a–d), excluding putative behavioral outcomes due to light-driven effects. In addition, when examining the response towards inanimate objects (Fig. s4a), *GAD2*^{Cre}::ChR2^{IPN} stimulation significantly decreased N-O investigation (Fig. s6a, c), while leaving exploration of a F-O intact (Fig. s6a–b). Consequently, the NP ratio was significantly reduced (Fig. s6d) without interfering with the total time of exploration (Fig. s6e). Importantly, neither photo-inhibition (Fig. s7a–d) nor photo-activation (Fig. s7e–h) of IPN GAD2 positive neurons altered anxiety-like behaviors. These data confirm that activation of IPN GABAergic neurons is both necessary and sufficient for reducing exploration towards familiar social and object stimuli, and therefore, the expression of NP.

To determine whether activation of the IPN and familiarity signaling is controlled by the major excitatory input innervating the IPN, which arises from medial habenula (mHb) cholinergic/glutamatergic neurons[18], we injected the mHb of mice expressing Cre under the control of the promoter for the gene encoding choline acetyltranferase, (*Chat*)*::Cre* mice with AAV2 encoding either NpHR3.0-eYFP or ChR2-eYFP and directly stimulated mHb axon terminals in the IPN (Fig. 3a–c). Cholinergic neurotransmission plays an important role in novelty processing[1] and familiarity-based responses[19], raising the possibility that cholinergic signaling in the IPN contributes to NP. We observed robust $eYFP^+$ expression in mHb cell bodies that colocalized with ChAT immunostaining (Fig. 3b) and abundant $eYFP^+$-axon bundles of the fasciculus retroflexus (fr) descending and innervating the dorsal and ventral central regions of the IPN (Fig. 3c). Optical stimulation of mHb $ChAT^+$ terminals in the IPN has previously been shown to evoke both glutamate and acetylcholine (ACh) release and enhance neural transmission[20,21]. Accordingly, electrophysiological recordings from mHb-IPN brain slices demonstrated that photo-activation of ChR2-expressing mHb $ChAT^+$ terminals in the IPN resulted in light-dependent increases in action potentials (APs) (Fig. 3d). In addition, photo-inhibition of the same terminals expressing NpHR reduced IPN neuronal activity (Fig. 3d). We investigated the $ChAT^+$ mHb→IPN functional connection on NP using previously established parameters of *in vivo* optogenetics for social (Fig. 2d) and inanimate (Fig. s4a) stimuli interactions. Optical stimulation of mHb cholinergic/glutamatergic terminals in the IPN (473 nm, 20 Hz, 12 ms pulse for 5 min) decreased exploration of N-S (Fig. 3e, g) and N-O stimuli (Fig. s8a, c) compared to control mice (light-OFF), mimicking familiar stimuli exploration-like responses, but did not interfere with F-S (Fig. 3e–f) or F-O investigation (Fig. s8a–b). The net $Chat^{Cre}$::$ChR2^{mHb→IPN}$ effect resulted in overall significantly decreased NP ratio for social (Fig. 3h) and inanimate stimuli (Fig. s8d). These results were not attributable to non-specific effects of light-stimulation (Fig. s9a–d). Conversely, $Chat^{Cre}$::$NpHR^{mHb→IPN}$ photo-inhibition (593 nm, constant light, 20 s ON, 10 s OFF) of mHb cholinergic/glutamatergic IPN terminals in $Chat^{Cre}$::$NpHR^{mHb→IPN}$ mice increased interest towards F-S (Fig. 3j–k) and F-O stimuli (Fig. s8g–h), mimicking exploration of novel-stimuli. Investigation of N-S (Fig. 3j, l) or N-O stimuli (Fig. s8g, i) were not affected by photo-inhibition of cholinergic/glutamatergic IPN terminals, altogether significantly decreasing the ratio of NP for social (Fig. 3m) or inanimate events (Fig. s8j). Activation (in $Chat^{Cre}$::$ChR2^{mHb→IPN}$ mice) or inhibition (in $Chat^{Cre}$::$NpHR^{mHb→IPN}$ mice) of mHb→IPN inputs did not significantly impact total time of investigation (Fig. 3i, n; Fig. s8e, k) or locomotor activity (Fig. s8f, l). Taken together, these data indicate that the mHb→IPN circuit bi-directionally modulates the saliency of novel vs. familiar stimuli and is both necessary and sufficient for the expression of NP.

Given that 1) novelty responses are mediated by VTA DAergic activity[10], 2) the IPN is located ventral-medial to the VTA, and 3) previous studies indicate the existence of a meso-interpeduncular circuit[22], we asked whether VTA DAergic neurons could potentially innervate the IPN to control NP. To this aim, we selectively expressed Cre-dependent ChR2-eYFP in the VTA of mice expressing Cre under the control of the promoter for *Slc6a3*, the gene encoding the DA transporter (DAT)*::Cre* mice via AAV2-mediated gene delivery (Fig. 4a) and observed VTA→IPN axonal projections (Fig. 4b). Axons arising from VTA DAergic neurons were more abundant in lateral and central regions of the caudal IPN (Fig.

s10a). To determine the functional contribution of $DA^{VTA\rightarrow IPN}$, we performed optogenetic circuit-specific terminal photo-stimulation in combination with slice electrophysiology. Whole-cell voltage-clamp recordings confirmed light-dependent inward currents in VTA ChR2-expressing DAergic cell bodies (Fig. s10b). Cell-attached recordings in caudal IPN neurons surrounded by eYFP-expressing VTA terminals revealed DAT^{Cre}::$ChR2^{VTA\rightarrow IPN}$ photo-stimulation elicited an increase in APs in 10/16 neurons which was completely blocked by pre-application of the D1 receptor antagonist SCH39166 (Fig. 4c–d), suggesting that activation of DAergic terminals leads to D1 receptor-dependent modulation of caudal IPN neuronal activity. In addition, *in vivo* photo-activation of presynaptic VTA DAergic terminals in the IPN triggered an overall reduced number of IPN Fos-positive neurons (Fig. s10c–d), suggesting these terminals may broadly inhibit IPN via activation of a small population of dopaminoceptive neurons to drive a novelty signal.

To investigate the functional consequences of DAT^{Cre}::$ChR2^{VTA\rightarrow IPN}$ neuronal firing in the responses to novel vs. familiar stimuli, we photo-stimulated IPN DAergic terminals during the social NP test (Fig. 4e). Stimulation was delivered in 30 Hz bursts of light (eight pulses, 5 ms each) every 5 s throughout the 5 min assay, a phasic pattern shown to evoke high levels of DA release[23]. DAT^{Cre}::$ChR2^{VTA\rightarrow IPN}$ phasic stimulation significantly increased F-S investigation (Fig. 4f–g), mimicking a novelty response. In contrast, N-S investigation remained intact (Fig. 4f, h), altogether resulting in a significantly reduced NP ratio compared to control animals without light delivery (Fig. 4i) or to animals injected with non-opsin, eYFP-encoding virus and receiving photo-illumination (Fig. s10e–h). Total exploratory behavior (Fig. 4j) or locomotion (Fig. 4k) was not affected by manipulating $DA^{VTA\rightarrow IPN}$ activity. When examining responses to inanimate objects (Fig. s11a), DAT^{Cre}::$ChR2^{VTA\rightarrow IPN}$ photo-activation did not significantly affect either F-O (Fig. s11b–c) nor N-O investigation (Fig. s11b, d), the NP ratio (Fig. s11e) or total exploratory behavior (Fig. s11f).

If, under social novelty circumstances, the VTA provides a DA signal in the IPN, this suggests IPN neurons may express DA receptors and these neurons should respond to novel social information. Our recordings from caudal IPN slices demonstrated D1 is critical in DAT^{Cre}::$ChR2^{VTA\rightarrow IPN}$ transmission and previous reports indicate D1 responses are linked to NP[23,24], together implying IPN D1 activity may be important for the expression of NP. We examined transgenic $Drd1a^{tdTomato}$ mice that use the mouse *Drd1a* gene promoter to drive the expression of DsRed fluorescent protein and found a rostro-caudal gradient in the relatively sparse density of D1-positive cell bodies in the IPN (Fig. 5a–b). Intra-IPN infusion of the D1 agonist SKF82958 elicited an increase in Fos expression in the majority of IPN D1-positive neurons, confirming a functional IPN response to DAergic input (Fig. s11g–h). To test how the IPN D1 neural subpopulation responds to novel and familiar events, $Drd1a^{tdTomato}$ encountered either F-S or N-S stimuli as represented in Fig 1a. F-S $Drd1a^{tdTomato}$ showed elevated numbers of Fos-positive nuclei in the IPN, as compared to the N-S group (Fig. 5c–d). However, a high number of Fos nuclei colocalized with DsRed fluorescence only in N-S $Drd1a^{tdTomato}$ (Fig. 5c, e), indicating activation of sparse IPN D1-positive neurons occurs upon exposure to novel but not familiar social conditions. Finally, to examine whether IPN D1 activity contributes to the expression of social NP, we pre-infused the D1-like family antagonist SCH39166 before phasic DAT^{Cre}::$ChR2^{VTA\rightarrow IPN}$ stimulation

(Fig. 5f–g). SCH39166 attenuated increased investigation towards F-S stimuli elicited by DAT^{Cre}::$ChR2^{VTA\rightarrow IPN}$ photo-stimulation (Fig. 5h–i), without significantly affecting N-S investigation (Fig. 5h, j), and increased the NP ratio to a more positive value (Fig. 5k). Pre-infusion of the drug did not alter total time of exploration (Fig. 5l). These results implicate the meso-interpeduncular circuit as a key modulator of NP through D1-receptor signaling in the IPN.

Discussion

Taken together, our data indicate that IPN GABAergic neuron activity is modulated by coordinated habenular cholinergic/glutamatergic and VTA DAergic neuron input, to form a critical circuit-based mechanism mediating the signaling of familiarity and the expression of NP. As opposed to dopaminergic midbrain areas that are activated by novel stimuli[9], overall IPN neuronal activity is progressively increased with multiple exposures to the same stimulus (F-S and F-O) as the stimulus becomes familiar, but reduces activity when interactions occur with novel stimuli (N-S and N-O). Optogenetic activation of IPN GABAergic neurons can inhibit investigation of a novel stimulus mimicking familiarity; whereas inhibition of these neurons induces increased investigation towards familiar stimuli without affecting exploration of a true novel stimulus, highlighting that the IPN is a critical node for familiarity signaling. Thus, when given a choice between novel and familiar stimuli, the IPN acts as a brake which is necessary and sufficient for reduced exploration of a familiar, but not novel signal to control NP. Importantly, the results from single object/social encounters and the CPP assay demonstrate that the IPN controls NP by assigning the salience of novel versus familiar information, as opposed to the *discrimination* of novel versus familiar stimuli, which presumably is mediated by cortical[25] and hippocampal[26] areas. In particular, reducing activation of the IPN during the CPP assay increases the rewarding properties of a familiar social encounter to that of a novel encounter; whereas, stimulation of IPN neurons reduces the rewarding value of novel social stimuli (data not shown), suggesting that the IPN controls the valence of motivation towards familiarity.

Stimulating or inhibiting excitatory mHb cholinergic/glutamatergic axon terminals in IPN bi-directionally controls NP similarly compared to direct IPN GABAergic neuron activation or silencing, indicating that the mHb acts upstream of the IPN to mediate familiarity-based responses. The mHb receives most afferent projections from the septum[27], which may provide encoded familiarity-based information. Via its projections to the IPN, the mHb represents a link between the forebrain and midbrain regions involved in reward and emotional processing[28]. Therefore, the mHb→IPN circuit could contribute to the cholinergic network extensively implicated in evaluation of novel vs. familiar information[29].

Several behaviors have been attributed to the mHb→IPN axis, including anxiety[30,31], fear-related responses[31–33] aversive memories[12], nicotine aversion[34,35] or withdrawal[21,22,36], most requiring conditioned learning or drug exposure. We exclude the possibility our results could be attributed to fear responses on the basis that our experimental procedures did not employ conditioned learning assays but instead utilized innate exploratory behavior. Furthermore, with manipulation of IPN activity, animals did not remain immobile, but

continued exploring, redirecting their levels of investigation exclusively towards familiar or novel stimuli.

Recent data indicate that there may be direct synaptic connectivity between the VTA and IPN[22]. Importantly, DAergic responses are linked to stimulus saliency as SN/VTA functional connectivity provide integrative information about novelty and reward[10]. Our study provides the first functional evidence that VTA DAergic neurons, specifically, innervate the IPN and modulate IPN neuronal activity to control novel vs. familiar interactions through novelty-induced activation of D1 receptor-expressing IPN neurons. While familiarity increases IPN activation overall, a relatively restricted sub-population of dopaminoceptive IPN neurons is activated by novel stimuli and selective activation of DAergic VTA→IPN input specifically increased investigation of a familiar social stimulus, essentially mimicking novelty-like exploration, an effect blocked by IPN infusion of a D1 receptor antagonist. These data raise the interesting possibility that the IPN controls familiarity signaling and NP through two distinct inputs: Familiarity signaling is received from the mHb which activates GABAergic IPN neurons to reduce the salience of once novel stimuli become familiar, thereby reducing exploration; whereas, novelty signaling is received from VTA DAergic neurons, activating a discreet dopaminoceptive IPN neuron population to presumably reduce activity of familiar signaling IPN neurons, enhancing salience and increasing exploration toward novel stimuli. Future studies will focus on further characterization of the neuronal identity and projection pattern of IPN dopaminoceptive neurons to determine if their activation by novel stimuli directly inhibits activity of familiarity-signaling IPN neurons, or if these neurons project to novelty-associated brain areas outside the IPN.

Interestingly, we found that stimulation of VTA→IPN DAergic terminals is sufficient to control the expression of NP for social but not inanimate stimuli. This is consistent with recent work indicating optogenetic activation of VTA DAergic neurons enhances social interaction with novel stimuli without affecting novel object interaction, despite *in vivo* imaging data indicating that VTA DAergic neuron activity is modulated by novel social *and* object interactions[9,37]. This result likely reflects the circuitry complexity and raises the possibility that other VTA neuronal subtypes mediate responses to non-social novel stimuli.

In summary, we have identified a previously unknown functional role for the IPN as a neuroanatomical substrate for familiarity signaling, together with convergent inputs from the mHb and VTA. To our knowledge, this is the first report indicating that information regarding familiar and novel stimuli signal through independent, yet connected circuits that affect familiarity signaling directly to control NP. Of note, we expect that dysregulation of familiarity signaling within IPN and associated circuits could play a role in neuropsychiatric disorders characterized by impaired novelty/familiarity interactions such as schizophrenia, autism, and addiction. Thus, targeting components of this circuit may provide novel therapeutic strategies for treating several neuropsychiatric conditions.

Online Methods

Animals

All experiments were conducted in accordance with the guidelines for care and use of laboratory animals provided by the National Research Council, as well as with an approved animal protocol from the Institutional Animal Care and Use Committee of the University of Massachusetts Medical School (UMMS). C57Bl/6J (#000664), *GAD2*^{Cre} (#10802), *Chat*^{Cre} (#006410), DAT^{Cre} (#006660) and *Drd1a*^{tdTomato} (#016204) mice were obtained from The Jackson Laboratory, bred in the UMMS animal facility and used in behavioral, optogenetic and biophysical experiments as indicated. Cre lines were crossed with C57Bl/6J mice and only heterozygous animals carrying one copy of the *Cre* recombinase gene were used for experimental purposes. For social experiments, juvenile stimuli always consisted of male C57Bl/6J mice (4–7 weeks old) bred in the UMMS animal facility. All mice were housed together and kept on a standard 12 h light/dark cycle (lights ON at 7 A.M.) with *ad libitum* access to food and water. Three to four weeks before experimentation, subject mice were kept under a reverse 12 h light/dark cycle (lights ON at 7 P. M.), and individually housed for at least 5 days before any behavioral testing.

Viral constructs

The pAAV-Ef1a-DIO-eNpHR3.0-eYFP, pAAV-Ef1a-DIO-ChR2-eYFP plasmids (generously provided by K. Deisseroth) and pAAV-Ef1a-DIO-eYFP (Addgene) were packaged into AAV serotype 2 (AAV_2) viral particles by the UMMS Viral Vector Core. AAV_2 was used as the serotype for all viral-mediated gene deliveries as AAV_2 preferentially infects neurons and exhibits minimal retrograde infection[38]. Viral titrations consisted of 8.5×10^{12} genome copies per ml for AAV2- Ef1a-DIO-eNpHR3.0-eYFP, 2.5×10^{12} viral particles per ml for pAAV-Ef1a-DIO-ChR2-eYFP and 5×10^{12} viral particles per ml for pAAV-Ef1a-DIO-eYFP. All viral injections were performed 4–6 weeks before experiments to allow for sufficient time for transgene expression.

Stereotaxic injections, cannula and optic fiber implantation

Surgery and injections were performed under aseptic conditions and stereotaxic guidance as previously described. Mice (6 – 8 weeks) were deeply anaesthetized using a 100 mg kg^{-1} ketamine (VEDCO) and 10 mg kg^{-1} xylazine (LLOYD) mixture. Following anesthesia treatment, a 0.4-mm drill was used for craniotomies at the target Bregma coordinates. All mice were microinjected at a controlled rate of 30 nl min^{-1} using a gas-tight 33G 10-µl neurosyringe (1701RN; Hamilton) in a microsyringe pump (Stoelting Co). After infusion, the needle remained in place for another 10 min before being slowly withdrawn. Injection placement coordinates were (in mm, Bregma anterioposterior (AP), mediolateral (ML), dorsoventral (DV) and angle): IPN (−3.4, −0.5, −4.82, 6°), VTA (−3.4, ±0.5, −4.5, 0°), mHb (−1.5, ±0.25, −2.8, 0°). Viral volumes for unilateral IPN and bilateral mHb injections were 300 nl, and 800 nl for bilateral VTA injections. For behavioral optogenetic experiments, 4 weeks post-injection, an unilateral optic fiber implant (200-µm core diameter; 0.53 NA, Doric Lenses) held in a magnetic aluminum receptacle (Doric Lenses) was placed above the IPN (−3.4, −0.5, −4.8, 6°) and secured into the skull using adhesive (C&B Metabond cement, Parkell Inc.) followed by dental cement (Cerebond, PlasticsOne). For

pharmacological experiments, a stainless steel guide cannula (23 gauge with 4-mm pedestals, PlasticsOne) was inserted above the IPN (−3.4, 0, −4.8, 0°) and secured to the skull with Cerebond. All mice received intraperitoneal (i.p.) injections of 1 mg kg^{-1} ketoprofen analgesic (Zoetis) and placed on heating pads until recovery from anesthesia. Mice were allowed to recover in their home cages for 5 days before any behavioral testing. Injection sites and viral expression were confirmed for all animals by experimenters blinded to behavioral outcome as previously described[30]. Animals showing no viral or off-target site viral expression or incorrect optic fiber placement were excluded from analysis. From a total of 206 mice, 34 mice were excluded from analysis due to incorrect viral expression or optic fiber placement.

Infusion of drug solutions

Mice were anesthetized with 2% isoflurane via a nose cone adaptor at a flow rate of 800 ml l^{-1}, as previously described[22]. An internal infusion cannula (30G) designed to reach IPN coordinates (−4.8 mm) was inserted into the guide cannula and vehicle (2% dimethyl sulfoxide, DMSO and 98% sterile saline) or D1 antagonist SCH39166 (70 ng μl^{-1} dissolved in 2% DMSO and 98% sterile saline) was infused at a rate of 0.3 µl min^{-1} for 1 min. After infusion, the injection cannula was left in place for an additional 2 min before removal. Subsequently, an optic fiber implant was inserted through the guide cannula and instant adhesive was used to stabilize the fiber to the cannula. SKF82958 (0.2 µg) was dissolved in sterile saline and also administered at a rate of 0.3 µl min^{-1}. The drug solutions were infused 10 min before behavioral testing. Animals showing incorrect cannula placement were excluded from analysis by experimenters blinded to treatment. From a total of 30 mice, 8 mice were excluded from analysis due to incorrect cannula placement.

Behavioral assays

All behavioral experiments were conducted during the active dark phase (8 A.M. to 6 P.M.) of mice aged between 9–12 weeks old. Animals were acclimated to the testing room for 30 min before any experiment, and all testing was performed under dim red light conditions. For experiments involving C57BL/6J and *Drd1a*^{tdTomato} mice, animals were used only in one behavioral paradigm. For optogenetic experiments, animals used for both social and object interactions underwent a minimum of at least a 4-day wash-out period between photo-stimulations. All social behavior experiments were performed in male mice that interacted with male juvenile stimuli. Data for object interaction using the *GAD2*^{Cre} line included both males and females as no sex differences were detected. All experiments were conducted in at least three cohorts of animals (i.e. in triplicate) which were randomly allocated into experimental groups and counterbalanced across cohorts.

Social interaction tests—For experiments involving C57BL/6J and *Drd1a*^{tdTomato} mice, social approach testing was performed using the standard three-chamber apparatus design as previously described[11]. The Plexiglas apparatus consisted of two identical compartments (each 42 × 24 × 30 cm) connected via a neutral central zone (42 × 15 × 30 cm) that allowed the animal to freely move between compartments. Each of the outer compartments contained an inverted plastic cylinder (14 cm × 11 cm diameter) with holes in it (1.5 cm diameter), allowing for direct physical contact (i.e. visual, gustatory, olfactory cues interaction)

between the stimulus and subject animals. Notably, in this protocol social approach is merely established by the testing animal, as juvenile mice are constrained inside a cup, thus removing the potential stress caused by any stimulus-directed physical contact[39]. Subject mice were first habituated to the apparatus for a 5-min period. Following habituation, a juvenile C57BL/6J mouse (4–7 weeks of age) was placed under one of the two inverted cylinders (counterbalanced). The subject mouse was then placed in the central zone and allowed to freely explore all three compartments for 5 min. This testing phase was repeated 24 h later on day 2, using the same juvenile mouse placed in the same compartment. Social investigation on days 1 and 2 was used to determine baseline exploratory behavior and to counterbalance sociability among subject animals. On day 3, half of the subject mice were presented for 5 min to the same familiar juvenile social stimulus as used on days 1 and 2, whereas the other half were presented to a new juvenile stimulus, located in the same compartment as on days 1 and 2. Interaction groups receiving a familiar or novel stimulus were balanced in an unbiased way to account for individual animals' social interest. A control group (Non-Social) was similarly presented to the apparatus and cylinders for three consecutive days, but never exposed to a social stimulus. For progressive social interactions, subject mice were presented for 5 min to the same familiar juvenile social stimulus and in the same cylinder for 7 consecutive days. All sessions were video recorded from above (HDR-CX4440 camera, SONY) and mouse behavior was tracked automatically using EthoVision XT 11.5 (Noldus Apparatus). Heat maps were generated in EthoVision XT with pseudo-color representing the relative time spent by the mouse at each position, with the maximum and minimum calculated within each session. Times exploring the social and non-social cylinders were manually scored by an experimenter blind to experimental conditions. Exploration was defined as real sniffing when a mouse directed its nose at a distance less than 2 cm from the cylinder. Sitting or resting next to the cylinder was not considered exploration. The social preference ratio was calculated as: (total social investigation – total non-social investigation)/(total investigation) over the 5 min session. The apparatus and cylinders were cleaned with Micro-90 solution (International Products Corporation) to eliminate olfactory traces after each session.

For optogenetic experiments, subject mice were tested in an open-field apparatus (42 × 38 × 30 cm) containing two plastic cylinders on opposite corners of the maze. Optic fiber implants were connected to a patch cable using magnetic force (Doric Lenses), which in turn was connected to a commutator (rotary joint; LEDFRJ-B_FC for blue light and LEDFRJ-A_FC for yellow light, Doric Lenses) by means of an FC/SMC adapter to allow unrestricted movement. On day 1, mice were subjected to a 5-min habituation session followed by a 5-min test session in which a juvenile mouse was placed inside one of the two cylinders (counterbalanced). This test session was repeated 24h later, with the same social stimulus located in the same cylinder. No light was delivered on days 1 and 2. Interaction groups receiving or not receiving photo-stimulation were balanced in an unbiased way to account for individual animals' social interest. On day 3, a familiar mouse (2 times encountered) was placed simultaneously with a novel juvenile stimulus in the opposite cylinder and half of the mice received paired optical stimulation (ChR2: 473 nm, 20 Hz, 12 ms pulse for 5 min; NpHR: 593 nm, constant light, 20 s ON, 10 s OFF for 5 min). The optogenetic parameters used for $DA^{VTA \rightarrow IPN}$ were consistent with a previously published protocol for DAergic

firing (8 pulses of 5 ms pulse-width, at 30 Hz, delivered every 5 s for 5 min)[17]. A high-power LED driver (DC2200, Thorlabs) was used to generate light pulses at intensity ~15–20 mW. A control group injected with Cre-dependent non-opsin virus (eYFP) was added to test light-derived effects and received the same optogenetic stimulation pattern as used for ChR2-injected animals. For these choice experiments, the preference ratio was calculated as: (total novel stimulus investigation – total familiar stimulus investigation)/(total investigation) over the 5 min session. For single presentations to social stimulus, similar experimental conditions were used. In this protocol, the subject mice encountered one juvenile social stimulus that remained the same and in the exact location (counterbalanced) for 4 consecutive days. On day 5, a novel juvenile stimulus was placed in that position. Half of the animals received paired photo-stimulation (NpHR: 593 nm, constant light, 20 s ON, 10 s OFF, ~15–20 mW, for 5 min) on days 3 and 5.

CPP test—The CPP apparatus (Med Associates) consisted of two outer conditioning chambers (each 13 × 15 × 12 cm) connected by a central neutral zone (13 × 10 × 12 cm). One chamber had black walls with a striped metal floor, and the other had white walls with a grid metal floor. For the novel social CPP, each chamber contained a plastic cylinder (9 cm × 7 cm diameter). The protocol consisted of three phases: pre-test, acquisition and test, all of them conducted under dim light and sound-attenuated conditions. During the pre-test phase, mice were placed in the central zone and allowed to explore the entire apparatus for 20 min. Conditioning groups were balanced in an unbiased fashion to account for potential baseline chamber preference. Five to six h after the pre-test session, subject mice were presented to a juvenile stimulus placed inside a cylinder in a neutral arena for 10 min. The acquisition phase consisted of three successive days with two conditioning trials each day separated 6 h apart. On days 2, 3 and 4 mice were confined to one chamber for 10 min while in the presence of either a familiar juvenile social stimulus (encountered in the neutral arena) or a novel juvenile stimulus (that changed every day) constrained inside a cylinder. Familiar and novel social stimuli were counterbalanced for conditioning chamber and morning/afternoon trials. Half of the subject mice were paired with photo-stimulation when presented to the familiar social stimulus on days 3 and 4 (NpHR: 593 nm, constant light, 20 s ON, 10 s OFF, ~15–20 mW, for 10 min). On the test day, subject mice were placed into the central zone area without social stimuli or light delivery and allowed to freely explore the apparatus for 20 min. Analysis of duration spent within either compartment was automatically recorded by MED-PC IV software (MED Associates Inc.). Subtracted CPP score was calculated as test phase duration spent in the social novel-paired chamber minus test-phase duration spent in the social familiar-paired chamber. For the real-time place-preference, mice were positioned in the central zone area and allowed to explore the entire apparatus for 20 min. Half of the animals did not receive light delivery and the absolute times spent in the left (L) and right (R) chambers were automatically measured. The other half of mice received light photo-stimulation (NpHR: 593 nm, constant light, ~15–20 mW) when they were present in either one of the two chambers (counterbalanced between animals), during the 20 min test duration.

Object interaction tests—The apparatus consisted of a T shaped maze (three arms, each 9 × 30 × 20 cm, connected through a central, 9 × 9 cm, zone) made of white Plexiglas. For

experiments using C57BL/6J mice, interest towards familiar and novel events was examined as described for social interaction but using inanimate objects instead of social stimuli, and in a T-maze context. Briefly, after 5 min of habituation to the apparatus, half of the mice were presented to an inanimate object located at one end of the T-maze arms (counterbalanced) for 5 min/day for three consecutive days. On day 3, the other half of mice were presented to a new inanimate object, placed in the same location as the previous object. All objects were plastic and induced similar levels of exploration. For optogenetic experiments, following 5 min of habituation, mice were presented to two inanimate objects positioned at each end of the T-maze arms. This session was repeated 24 h later. No light was delivered on days 1 and 2. On day 3, a novel object replaced one of the previous objects and half of the mice received paired optical stimulation (identical parameters as for social interactions). For single presentations to inanimate objects, all subject mice encountered one inanimate object that remained the same and in the same location for 2 consecutive days. No light was delivered on days 1 and 2. Interaction groups with either novel or familiar object stimuli were balanced in an unbiased way to account for individual animals' rates of investigation. On days 3 and 4, half the subject mice were presented to the same familiar object, whereas the other half encountered a novel inanimate object kept at the same position as before. Within the novel and familiar groups, half of the animals received paired photo-stimulation only on day 3 (identical parameters as for social interactions).

Open field—Mice were individually placed facing one of the walls of a Plexiglass open-field (42 × 38 × 30 cm). Mice were allowed to explore freely for 10 min and the time spent in the center of the chamber, as compared to the outer areas was automatically tracked using EthoVision XT 11.5 (Noldus Apparatus). Half of the animals received light stimulation for the entire 10-min session (with the same parameters as described above).

Marble burying—The test was performed in standard mouse cages filled with a 5 – 6-cm layer of bedding material. All mice were habituated to the test cages for two consecutive days (30 – 40 min per day) without light stimulation. On the third day, 15 sterilized 1.5-cm glass marbles were evenly spaced above the bedding in five rows of three, each 4 cm apart. Implanted mice were placed in the test cage and left for 20 min, and the number of marbles buried with bedding (to 2/3 their depth) was counted. Half of the animals received photo-illumination during the 20-min session.

Elevated plus maze—Implanted mice were plugged into a corresponding patch cord by magnetic force before the beginning of the session and subsequently placed in an elevated plus maze. The apparatus consisted of four arms connected by a central axis (5 × 5 cm) and was elevated 45 cm above the floor. Two of the arms were enclosed with plastic black walls (5× 30 × 15 cm) while the other two remained open (5 × 30 ×0.25 cm). At the start of each session, mice were placed at the intersection of the maze facing into an arm with no walls and allowed 5 min of free exploration. Optical stimulation occurred in half of the animals and during the entire 5-min session (with the same parameters as described above). The number of entries into the open and closed arms and the total time spent in the open and closed arms were measured by MED-PC IV software. The time spent in open arms was

considered an index of anxiety-like behavior and the total number of entries as an index of locomotor activity. The apparatus was cleaned between animals with Micro-90 solution.

Immunohistochemistry

Immunohistochemistry and microscopy were performed as described previously[36]. In brief, mice were given a euthanizing dose of sodium pentobarbital (200 mg kg^{-1}) and transcardially perfused with ice-cold 0.1 M phosphate buffer saline (PBS, pH 7.4) followed by 10 ml of cold 4% (W/V) paraformaldehyde (PFA) in 0.1 M PBS. Brains were post-fixed for 4h in 4% PFA and submerged in 30 % sucrose for 48h. Coronal sections (25 μm) were obtained using a freezing microtome (HM430; Thermo Fisher Scientific, MA, USA) to assess viral placement and immunohistochemistry. For immunohistochemical experiments, brain sections were permeabilized with 0.5% Triton X-100 in 0.1M PBS for 10 min, blocked with 5% donkey serum (DS, Sigma) in 0.1 M PBS for 30 min and then incubated overnight (o.n.) with the corresponding primary antibodies in 0.1 M PBS 3% DS at 4 °C. Primary antibodies used: rabbit anti Fos 1:700 (Santa Cruz Biotechnology, SC-42); mouse anti-TH 1:500 (Millipore, MAB318); rabbit anti-GAD1/2 1:1000 (Sigma, G5163), mouse anti-GAD2 1:800 (Sigma, G1166); goat anti-ChAT 1:400 (Millipore, AB144P). Slices were subsequently washed in 0.1M PBS and incubated in secondary antibodies for 2 h (1:800; Life Technologies; donkey anti-rabbit 488 (A21206); donkey anti-rabbit 594 (A21207); donkey anti-mouse 594 (A21203); goat anti-mouse 488 (A11017); donkey anti-goat 594 (A11058)). After washes in 0.1 M PBS, nuclei were counterstained with DAPI, sections were mounted, air-dried and coverslipped with Mowiol (Sigma). All slices were imaged using a fluorescent microscope (Zeiss, Carl Zeiss MicroImmagine, Inc., NY, USA) connected to computer-associated image analyzer software (Axiovision Rel., 4.6.1). All antibodies used have been verified previously for the intended use by the manufacturer. For Fos studies, fluorescent images were acquired at 20× magnification and analysis of Fos-positive nuclei was performed using Image J software. Fos-positive nuclei were counted in all IPN serial slices and averaged in each mouse. For colocalization analysis between Fos and GAD1/2, the percentage of colocalized nuclei was estimated by dividing the number of Fos positive nuclei also labeled with GAD1/2 staining versus the total number of Fos positive nuclei. All animals were perfused 90 min post-assay or optical stimulation. Optical stimulation was delivered for 5 min in mice while remaining in their home cages (ChR2: 473 nm, 8 pulses of 5 ms pulse-width, at 30 Hz, delivered every 5 s, ~15–20 mW).

Slice preparation and electrophysiology

For optogenetic slice electrophysiology, mice (10–12 weeks) were anesthetized by i.p. injection of sodium pentobarbital (200 mg/kg). Brains were quickly removed and placed in an oxygenated ice-cold cutting solution containing (in mM): 2.5 KCl, 1.25 $NaH_2PO_4•H_2O$, 20 HEPES, 2 Thiourea, 5 Na-ascorbate, 92 NMDG, 30 $NaHCO_3$, 0.5 $CaCl_2•2H_2O$ and 10 $MgSO_4•7H_2O$. Brain slices (180 ~ 200 μM) were made using a Leica VT1200 vibratome. For recordings in the IPN and VTA, coronal brain slices (~ 200 μm) containing these regions were obtained using a vibratome (VT1200, Leica). For verifying optogenetic control of mHb→IPN connections in *Chat*^{Cre} mice, hybrid brain sections containing both regions were prepared. Brain slices were incubated in oxygenated cutting solution at 34°C for 20 min. Slices were transferred into oxygenated artificial cerebrospinal fluid (ACSF) at room

temperature for recording. ACSF solution contains (in mM): 125 NaCl, 2.5 KCl, 1.2 $NaH_2PO_4•H_2O$, 1.2 $MgCl_2•6H_2O$, 2.4 $CaCl_2•2H_2O$, 26 $NaHCO_3$, 11 D-Glucose. Single slices were transferred into a recording chamber and continually superfused with oxygenated ACSF. The junction potential between the patch pipette and bath ACSF was nullified just before obtaining a seal. Action potentials were recorded at 32°C using the whole-cell configuration of a patch-clamp amplifier (Multiclamp 700B; Molecular Devices). Action potentials were obtained by an episodic or gap-free acquisition mode using Clampex software (Molecular Devices). Signals were filtered at 1 kHz using the amplifier's four-pole, low-pass Bessel filter, digitized at 10 kHz with a Digidata 1440A interface (Molecular Devices) and stored on a personal computer. Pipette solution contained (in mM) 121 KCl, 4 $MgCl_2•6H_2O$, 11 EGTA, 1 $CaCl_2•2H_2O$, 10 HEPES, 0.2 GTP, and 4 ATP. For optical recordings, eYFP-positive neurons or eYFP signal surrounding soma (for presynaptic stimulation) were identified under fluorescence microscopy. Light pulses at 593 nm (for NpHR) or 473 nm (for ChR2, 20Hz) were applied to neurons under current clamp or voltage clamp using LEDs of the appropriate wavelength (ThorLabs). For pharmacological experiments to block optogenetically-evoked DAergic responses, SCH39166 (10 μM) was added to the bath solution.

Statistics

Data were analyzed by means of two-tailed unpaired *t*-test, one-way or two-way ANOVAs or repeated-measures (RM) ANOVA as indicated, using Graphpad Software (Graphpad Software Inc.). Bonferroni was used as a *post hoc* test when appropriate for one-way and two-way ANOVAs. Unpaired *t*-test was used for choice paradigms to calculate differences between two groups in terms of familiar and novel stimuli investigation, preference ratio, total investigation time and total distance travelled. The t-test was also applied for the anxiety tests, Fos expression analysis between two groups and for the CPP experiment to calculate the effect of two different conditions. Two-way RM ANOVA was used for single interactions with familiar and novel stimuli across consecutive days when comparing two groups of mice, with day and group as main factors. One-way ANOVA was used for analysis of Fos expression in more than two groups of mice and in the choice experiments comprising three groups of animals. To analyze the changes in AP upon light delivery we used one-way RM ANOVA. Each data set was tested for normal distribution and equal variances prior to analysis and statistical significance was established at $p<0.05$. No statistical methods were used to pre-determine sample sizes but animal numbers were determined based on previous studies using similar endpoints[27]. All data are expressed as mean ± standard error of the mean (SEM).

Data Availability

The data that support the findings of this study are available from the corresponding author upon reasonable request.

Supplementary Material

Refer to Web version on PubMed Central for supplementary material.

Acknowledgments

We thank Dr. Karl Deisseroth for optogenetic plasmids and Dr. Guangping Gao for viral plasmid packaging. We also thank Anthony Sacino for technical support. This work was supported by the National Institute on Drug Abuse award number DA041482 (A.R.T.), DA035371 (P.D.G. and A.R.T.) and by a NARSAD Independent Investigator Grant from the Brain & Behavior Research Foundation (A.R.T.). The content is solely the responsibility of the authors and does not necessarily represent the official views of the National Institutes of Health.

References

1. Ranganath C, Rainer G. Neural mechanisms for detecting and remembering novel events. Nat Rev Neurosci. 2003; 4:193–202. DOI: 10.1038/nrn1052 [PubMed: 12612632]
2. Billeke P, Aboitiz F. Social cognition in schizophrenia: from social stimuli processing to social engagement. Front Psychiatry. 2013; 4:4. [PubMed: 23444313]
3. Weigelt S, Koldewyn K, Kanwisher N. Face identity recognition in autism spectrum disorders: a review of behavioral studies. Neurosci Biobehav Rev. 2012; 36:1060–1084. DOI: 10.1016/j.neubiorev.2011.12.008 [PubMed: 22212588]
4. Tegelbeckers J, et al. Altered salience processing in attention deficit hyperactivity disorder. Hum Brain Mapp. 2015; 36:2049–2060. DOI: 10.1002/hbm.22755 [PubMed: 25648705]
5. Buchel C, et al. Blunted ventral striatal responses to anticipated rewards foreshadow problematic drug use in novelty-seeking adolescents. Nature communications. 2017; 8:14140.
6. Wingo T, Nesil T, Choi JS, Li MD, Novelty Seeking. Drug Addiction in Humans and Animals: From Behavior to Molecules. J Neuroimmune Pharmacol. 2016; 11:456–470. DOI: 10.1007/s11481-015-9636-7 [PubMed: 26481371]
7. Lisman JE, Otmakhova NA. Storage, recall, and novelty detection of sequences by the hippocampus: elaborating on the SOCRATIC model to account for normal and aberrant effects of dopamine. Hippocampus. 2001; 11:551–568. DOI: 10.1002/hipo.1071 [PubMed: 11732708]
8. Hitti FL, Siegelbaum SA. The hippocampal CA2 region is essential for social memory. Nature. 2014; 508:88–92. DOI: 10.1038/nature13028 [PubMed: 24572357]
9. Bunzeck N, Duzel E. Absolute coding of stimulus novelty in the human substantia nigra/VTA. Neuron. 2006; 51:369–379. DOI: 10.1016/j.neuron.2006.06.021 [PubMed: 16880131]
10. Krebs RM, Heipertz D, Schuetze H, Duzel E. Novelty increases the mesolimbic functional connectivity of the substantia nigra/ventral tegmental area (SN/VTA) during reward anticipation: Evidence from high-resolution fMRI. Neuroimage. 2011; 58:647–655. DOI: 10.1016/j.neuroimage.2011.06.038 [PubMed: 21723396]
11. Moy SS, et al. Sociability and preference for social novelty in five inbred strains: an approach to assess autistic-like behavior in mice. Genes Brain Behav. 2004; 3:287–302. DOI: 10.1111/j.1601-1848.2004.00076.x [PubMed: 15344922]
12. Soria-Gomez E, et al. Habenular CB1 Receptors Control the Expression of Aversive Memories. Neuron. 2015; 88:306–313. DOI: 10.1016/j.neuron.2015.08.035 [PubMed: 26412490]
13. Chou MY, et al. Social conflict resolution regulated by two dorsal habenular subregions in zebrafish. Science. 2016; 352:87–90. DOI: 10.1126/science.aac9508 [PubMed: 27034372]
14. Cole AJ, Saffen DW, Baraban JM, Worley PF. Rapid increase of an immediate early gene messenger RNA in hippocampal neurons by synaptic NMDA receptor activation. Nature. 1989; 340:474–476. [PubMed: 2547165]
15. Hemmendinger LM, Moore RY. Interpeduncular nucleus organization in the rat: cytoarchitecture and histochemical analysis. Brain Res Bull. 1984; 13:163–179. [PubMed: 6148133]
16. Gradinaru V, et al. Molecular and cellular approaches for diversifying and extending optogenetics. Cell. 2010; 141:154–165. DOI: 10.1016/j.cell.2010.02.037 [PubMed: 20303157]
17. Tsai HC, et al. Phasic firing in dopaminergic neurons is sufficient for behavioral conditioning. Science. 2009; 324:1080–1084. doi:1168878 [pii]10.1126/science.1168878. [PubMed: 19389999]
18. Woolf NJ, Butcher LL. Cholinergic systems in the rat brain: II. Projections to the interpeduncular nucleus. Brain Res Bull. 1985; 14:63–83. [PubMed: 2580607]

19. Eckart C, Wozniak-Kwasniewska A, Herweg NA, Fuentemilla L, Bunzeck N. Acetylcholine modulates human working memory and subsequent familiarity based recognition via alpha oscillations. Neuroimage. 2016; 137:61–69. DOI: 10.1016/j.neuroimage.2016.05.049 [PubMed: 27222217]
20. Ren J, et al. Habenula "cholinergic" neurons co-release glutamate and acetylcholine and activate postsynaptic neurons via distinct transmission modes. Neuron. 2011; 69:445–452. doi:S0896-6273(10)01088-3 [pii] 10.1016/j.neuron.2010.12.038. [PubMed: 21315256]
21. Frahm S, et al. An essential role of acetylcholine-glutamate synergy at habenular synapses in nicotine dependence. Elife. 2015; 4:e11396. [PubMed: 26623516]
22. Zhao-Shea R, et al. Increased CRF signalling in a ventral tegmental area-interpeduncular nucleus-medial habenula circuit induces anxiety during nicotine withdrawal. Nature communications. 2015; 6:6770.
23. Adamantidis AR, et al. Optogenetic interrogation of dopaminergic modulation of the multiple phases of reward-seeking behavior. J Neurosci. 2011; 31:10829–10835. DOI: 10.1523/JNEUROSCI.2246-11.2011 [PubMed: 21795535]
24. Loiseau F, Millan MJ. Blockade of dopamine D(3) receptors in frontal cortex, but not in sub-cortical structures, enhances social recognition in rats: similar actions of D(1) receptor agonists, but not of D(2) antagonists. Eur Neuropsychopharmacol. 2009; 19:23–33. DOI: 10.1016/j.euroneuro.2008.07.012 [PubMed: 18793829]
25. Ho JW, et al. Bidirectional Modulation of Recognition Memory. J Neurosci. 2015; 35:13323–13335. DOI: 10.1523/JNEUROSCI.2278-15.2015 [PubMed: 26424881]
26. Okuyama T, Kitamura T, Roy DS, Itohara S, Tonegawa S. Ventral CA1 neurons store social memory. Science. 2016; 353:1536–1541. DOI: 10.1126/science.aaf7003 [PubMed: 27708103]
27. Qin C, Luo M. Neurochemical phenotypes of the afferent and efferent projections of the mouse medial habenula. Neuroscience. 2009; 161:827–837. DOI: 10.1016/j.neuroscience.2009.03.085 [PubMed: 19362132]
28. Sutherland RJ. The dorsal diencephalic conduction system: a review of the anatomy and functions of the habenular complex. Neurosci Biobehav Rev. 1982; 6:1–13. [PubMed: 7041014]
29. Bunzeck N, Guitart-Masip M, Dolan RJ, Duzel E. Pharmacological dissociation of novelty responses in the human brain. Cereb Cortex. 2014; 24:1351–1360. DOI: 10.1093/cercor/bhs420 [PubMed: 23307638]
30. Pang X, et al. Habenula cholinergic neurons regulate anxiety during nicotine withdrawal via nicotinic acetylcholine receptors. Neuropharmacology. 2016; 107:294–304. DOI: 10.1016/j.neuropharm.2016.03.039 [PubMed: 27020042]
31. Yamaguchi T, Danjo T, Pastan I, Hikida T, Nakanishi S. Distinct roles of segregated transmission of the septo-habenular pathway in anxiety and fear. Neuron. 2013; 78:537–544. DOI: 10.1016/j.neuron.2013.02.035 [PubMed: 23602500]
32. Agetsuma M, et al. The habenula is crucial for experience-dependent modification of fear responses in zebrafish. Nat Neurosci. 2010; 13:1354–1356. DOI: 10.1038/nn.2654 [PubMed: 20935642]
33. Zhang J, et al. Presynaptic Excitation via GABAB Receptors in Habenula Cholinergic Neurons Regulates Fear Memory Expression. Cell. 2016; 166:716–728. DOI: 10.1016/j.cell.2016.06.026 [PubMed: 27426949]
34. Fowler CD, Lu Q, Johnson PM, Marks MJ, Kenny PJ. Habenular alpha5 nicotinic receptor subunit signalling controls nicotine intake. Nature. 2011; 471:597–601. doi:nature09797 [pii]10.1038/nature09797. [PubMed: 21278726]
35. Frahm S, et al. Aversion to nicotine is regulated by the balanced activity of beta4 and alpha5 nicotinic receptor subunits in the medial habenula. Neuron. 2011; 70:522–535. doi:S0896-6273(11)00339-4 [pii]10.1016/j.neuron.2011.04.013. [PubMed: 21555077]
36. Zhao-Shea R, Liu L, Pang X, Gardner PD, Tapper AR. Activation of GABAergic neurons in the interpeduncular nucleus triggers physical nicotine withdrawal symptoms. Curr Biol. 2013; 23:2327–2335. DOI: 10.1016/j.cub.2013.09.041 [PubMed: 24239118]
37. Gunaydin LA, et al. Natural neural projection dynamics underlying social behavior. Cell. 2014; 157:1535–1551. DOI: 10.1016/j.cell.2014.05.017 [PubMed: 24949967]

38. Shevtsova Z, Malik JM, Michel U, Bahr M, Kugler S. Promoters and serotypes: targeting of adeno-associated virus vectors for gene transfer in the rat central nervous system in vitro and in vivo. Exp Physiol. 2005; 90:53–59. [PubMed: 15542619]

39. Silverman JL, Yang M, Lord C, Crawley JN. Behavioural phenotyping assays for mouse models of autism. Nat Rev Neurosci. 2010; 11:490–502. DOI: 10.1038/nrn2851 [PubMed: 20559336]

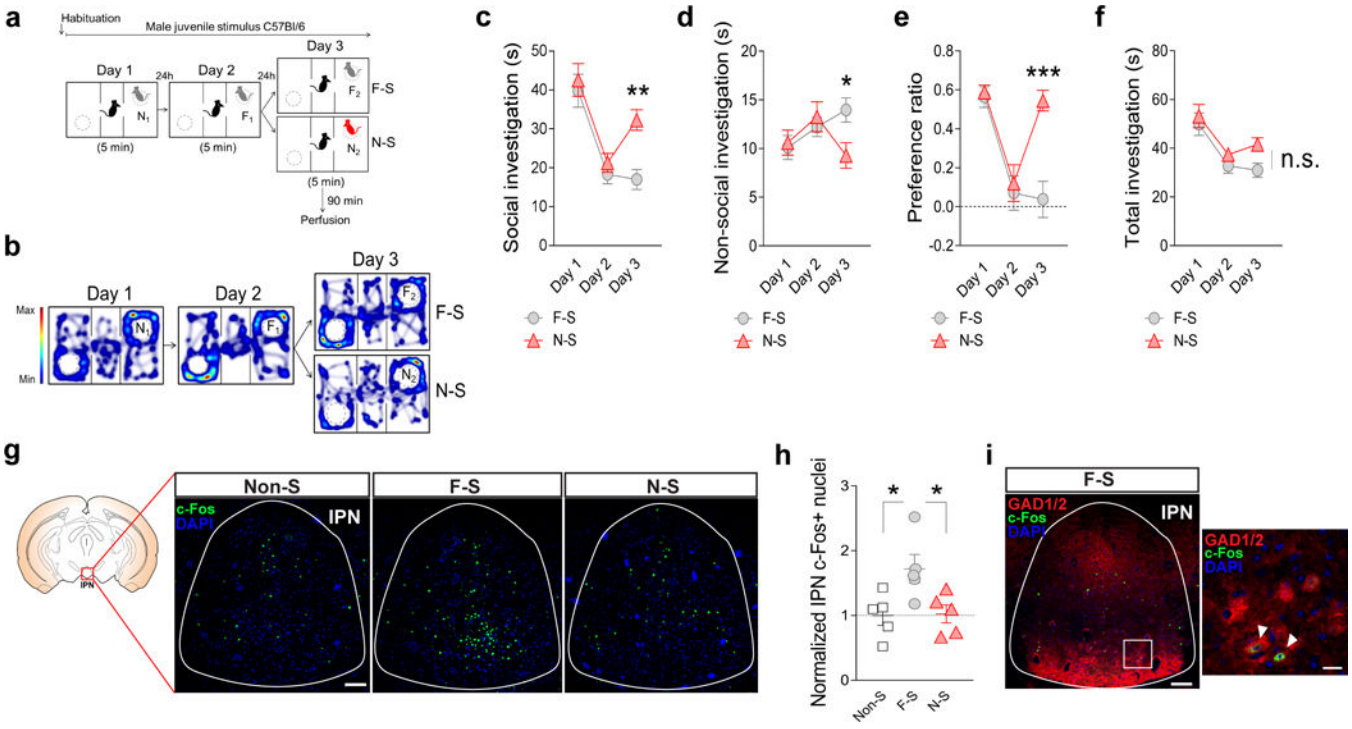

Figure 1. Familiar and novel social encounters differentially activate the IPN

(**a**) Schematic of experimental approach used to measure interactions with F-S (n = 20 mice) and N-S stimuli (n = 16 mice). Mice were exposed to the same juvenile on day 1 (N_1) and 2 (F_1). On day 3 mice were split into two groups and were exposed either to the same juvenile (F_2) or a new juvenile (N_2). (**b**) Representative spatial heat maps showing the location of the test mouse each day of the social interaction test. (**c**) Time spent investigating the social cylinder decreased across consecutive days (two-way repeated-measures (RM) ANOVA, day effect $F_{2,68} = 41.31$, $p < 0.0001$). Exposure to a new juvenile increased social investigation (day × stimulus group interaction $F_{2,68} = 4.22$, $p = 0.0187$; post-hoc test, **p = 0.0035). (**d**) Time spent investigating the non-social cylinder decreased in the N-S group (two-way RM ANOVA, day × stimulus group interaction $F_{2,68} = 3.95$, $p = 0.0239$; post-hoc test, *p = 0.0311). (**e**) Preference ratio for a social stimulus decreased across consecutive days (two-way RM ANOVA, day effect $F_{2,68} = 23.32$, $p < 0.0001$) but rebounded in the N-S group (day × stimulus group interaction $F_{2,68} = 7.35$, $p = 0.0013$; post-hoc test, ***p < 0.0001). (**f**) Total investigation time decreased across days (two-way RM ANOVA, day effect $F_{2,68} = 24.43$, $p < 0.0001$) but similarly between groups (day × stimulus group interaction $F_{2,68} = 1.10$, $p = 0.3382$). (**g**) Representative images of Fos immunoreactivity in coronal sections containing the IPN. Scale bar 50 μm. IPN, interpeduncular nucleus. (**h**) Normalized Fos immunopositive nuclei in the IPN from mice encountering a familiar (F_2) social stimulus (F-S) were significantly higher than control animals (no social encounters, Non-S), or mice encountering a novel (N_2) social stimulus (N-S) (one-way ANOVA $F_{2,12} = 5.49$, $p = 0.0203$; post-hoc test, *p = 0.0385 and *p = 0.0466; n = 5 mice per group). (**i**) Representative image of GAD1/2 (red) and Fos (green) immunofluorescence in the IPN of the F-S group. Arrowheads show colocalized nuclei (inset). Nuclei were labeled with DAPI (blue). Scale

bars (50 μm left panel; 20 μm right panel). Data are expressed as mean ± s.e.m., n.s. no significant.

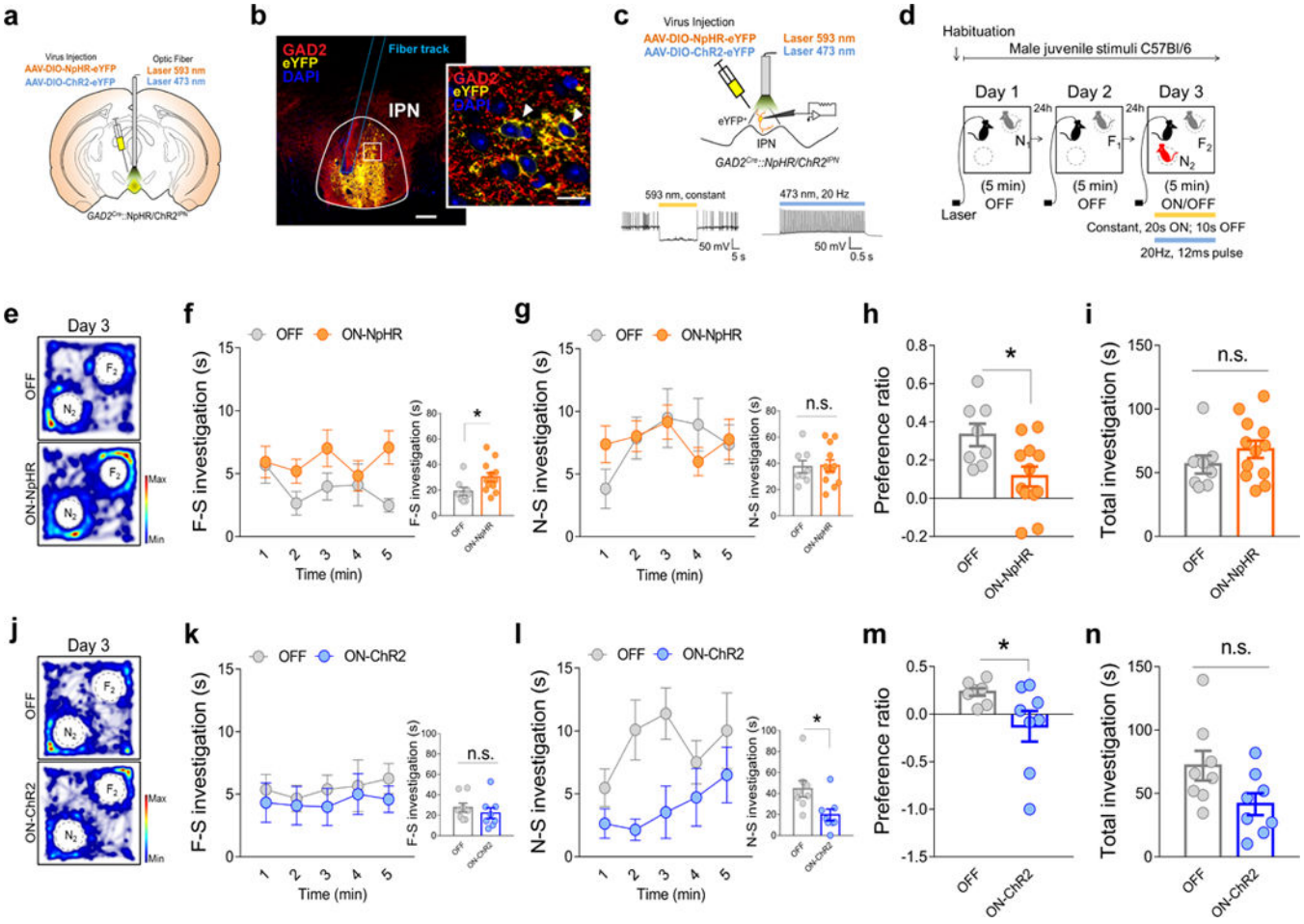

Figure 2. IPN GABAergic activity bi-directionally modulates social NP

(**a**) Schematic of optogenetic injections and optic stimulation strategies used. (**b**) Representative midbrain coronal section from a *GAD2*^{Cre} mouse infected with AAV2-DIO-NpHR-eYFP in the IPN (yellow) and GAD2 immunostaining (red). Nuclei were labeled with DAPI (blue). Arrowheads show colocalized neurons (inset). The coronal section shown was processed after *in vivo* optogenetic silencing (note optic fiber track placement in the IPN). Scale bars (100 μm left panel; 20 μm right panel). (**c**) Top: experimental configuration for verification of functional ChR2 and NpHR expression. Bottom: representative traces from eYFP^{+} IPN current-clamped neurons in midbrain slices demonstrate light-induced silencing (left trace) or activation (right trace) during NpHR^{IPN} and ChR2^{IPN} photo-stimulation, respectively. (**d**) Schematic of experimental approach used for determining interactions with F-S and N-S stimuli in the social NP task. For *GAD2*^{Cre}::NpHR^{IPN} mice: (**e**) representative heat maps showing the location of testing mice during the social NP task under light-OFF (top) (n = 8 mice) or light-ON conditions (bottom) (n = 12 mice). (**f**) Time of F-S investigation each minute of the social NP task was higher in the light-ON conditions. (Inset) Average total time of F-S investigation (unpaired *t*-test, $t_{18} = 2.25$, *p = 0.0371). (**g**) Time of N-S investigation each minute in the social NP task. (Inset) Average total time of N-S investigation (unpaired *t*-test, $t_{18} = 0.13$: p = 0.9011). (**h**) Novelty preference ratio was reduced during light-induced photo-inhibition (unpaired *t*-test, $t_{18} = 2.72$, *p = 0.0141). (**i**)

Total investigation time remained unaffected by the light (unpaired *t*-test, $t_{18} = 1.17$, p = 0.2575). For *GAD2*^{Cre}::ChR2^{IPN} mice: (**j**) representative heat maps showing the location of testing mice during the social NP task under light-OFF (top) (n = 8 mice) and light-ON conditions (bottom) (n = 8 mice). (**k**) Time of F-S investigation each minute of the social NP task. (Inset) Average total time of F-S investigation (unpaired *t*-test, $t_{14} = 0.78$, p = 0.4471). (**l**) Time of N-S investigation each minute of the social NP task. (Inset) Average total time of N-S investigation (unpaired *t*-test, $t_{14} = 2.60$, *p =0.0208). (**m**) Preference ratio decreased in the light-ON group (unpaired *t*-test, $t_{14} = 2.16$, *p = 0.0484) without affecting (**n**) total investigation time (unpaired *t*-test, $t_{14} = 2.08$, p = 0.0561). Data are expressed as mean ± s.e.m., n.s. not significant.

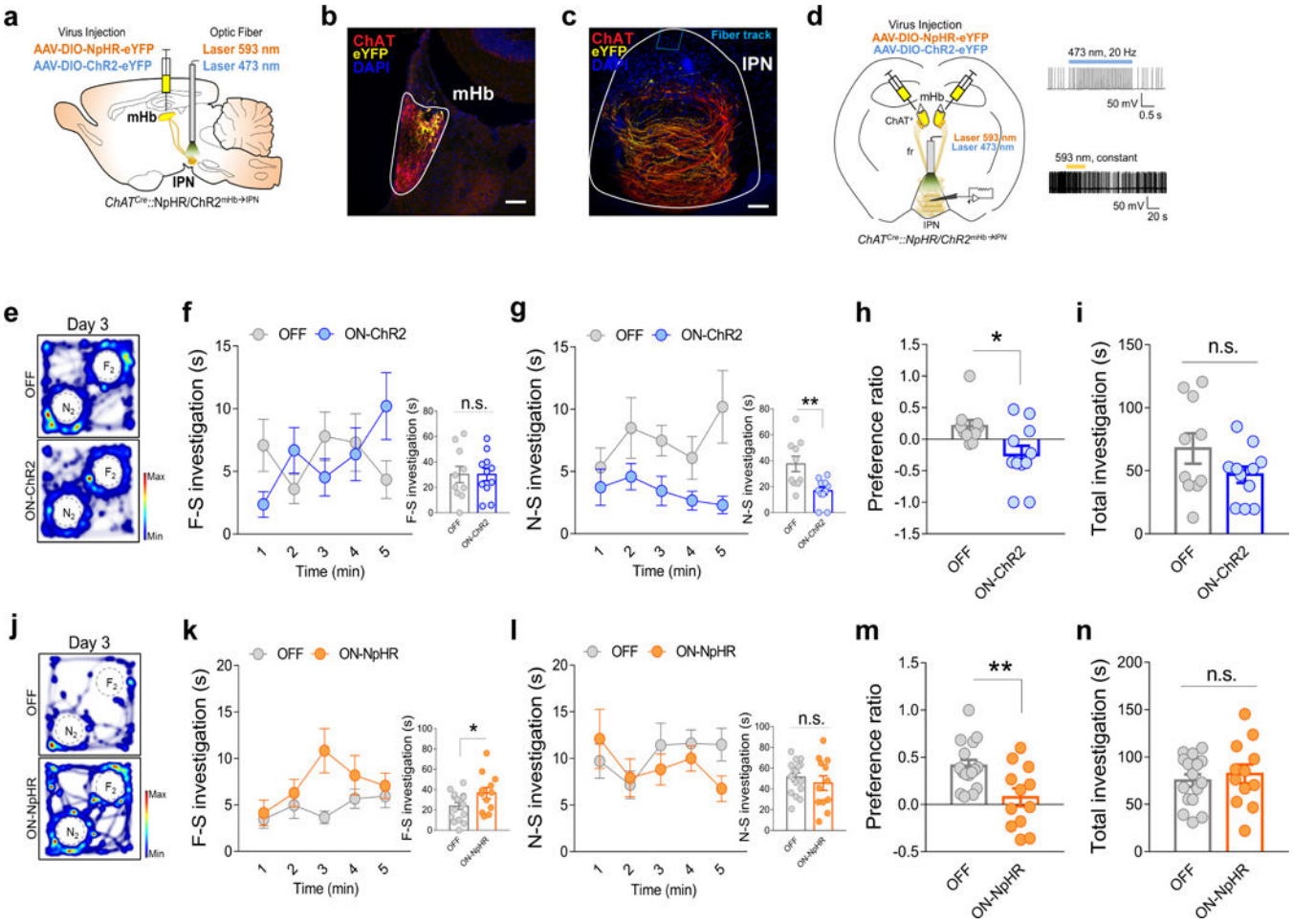

Figure 3. mHb cholinergic/glutamatergic input in IPN bi-directionally modulates social NP

(**a**) Schematic of optogenetic injections in the mHb and optic stimulation strategy in the IPN of *Chat*^{Cre} mice. (**b**) Representative epithalamic coronal section from a *Chat*^{Cre} mouse infected with AAV2-DIO-ChR2-eYFP in the mHb. MHb ChR2-eYFP expression (yellow signal) is co-localized with ChAT immunostaining (red signal). Nuclei were labeled with DAPI (blue signal). Scale bar 50 μm. (**c**) Representative image of eYFP^{+} axon bundles innervating the IPN and immunolabeled for ChAT staining (red signal). Scale bar 50 μm. (**d**) Left: experimental configuration for verification of functional ChR2 and NpHR expression. Right: representative traces from IPN current-clamped neurons in transverse epithalamic-midbrain slices demonstrate light-induced activation (top trace) or inhibition (bottom trace) during ChR2$^{mHb\rightarrow IPN}$ and NpHR$^{mHb\rightarrow IPN}$ synaptic photo-stimulation, respectively. In *Chat*^{Cre}::ChR2$^{mHb\rightarrow IPN}$ mice: (**e**) representative heat maps showing the location of testing mice in control (light-OFF, top)(n = 10 mice) and light-ON conditions (bottom)(n = 11 mice). (**f**) Time spent investigating F-S stimuli each minute of the social NP task. (Inset) Average total time of F-S investigation (unpaired *t*-test, $t_{19} = 0.00$, p = 0.9966). (**g**) Time spent investigating N-S stimuli each minute of the social NP task. (Inset) Average total time of N-S investigation (unpaired *t*-test, $t_{19} = 3.26$, **p = 0.0041). (**h**) Social NP ratio decreased during light-induced photo-stimulation (unpaired *t*-test, $t_{19} = 2.57$, *p = 0.0188) without affecting (**i**) total investigation time (unpaired *t*-test, $t_{19} = 1.59$, p = 0.1334). In

Chat^{Cre}::NpHR$^{mHb\rightarrow IPN}$ mice: (**j**) representative heat maps showing the location of testing mice in control (light-OFF, top)(n = 16 mice) and light-ON conditions (bottom) (n = 12 mice). (**k**) Time spent investigating F-S stimuli each minute of the social NP task. (Inset) Average total time of F-S investigation (unpaired *t*-test, $t_{26} = 2.10$, *p = 0.0452). (**l**) Time spent investigating N-S stimuli each minute of the social NP task. (Inset) Average total time of N-S investigation (unpaired *t*-test, $t_{26} = 0.76$, p = 0.4527). (**m**) Social NP ratio decreased in mice receiving photo-inhibition (unpaired *t*-test, $t_{26} = 3.03$, **p =0.0055) without interfering with (**n**) total investigation time (unpaired *t*-test, $t_{26} = 0.61$, p = 0.5441). Data are expressed as mean ± s.e.m., n.s. not significant.

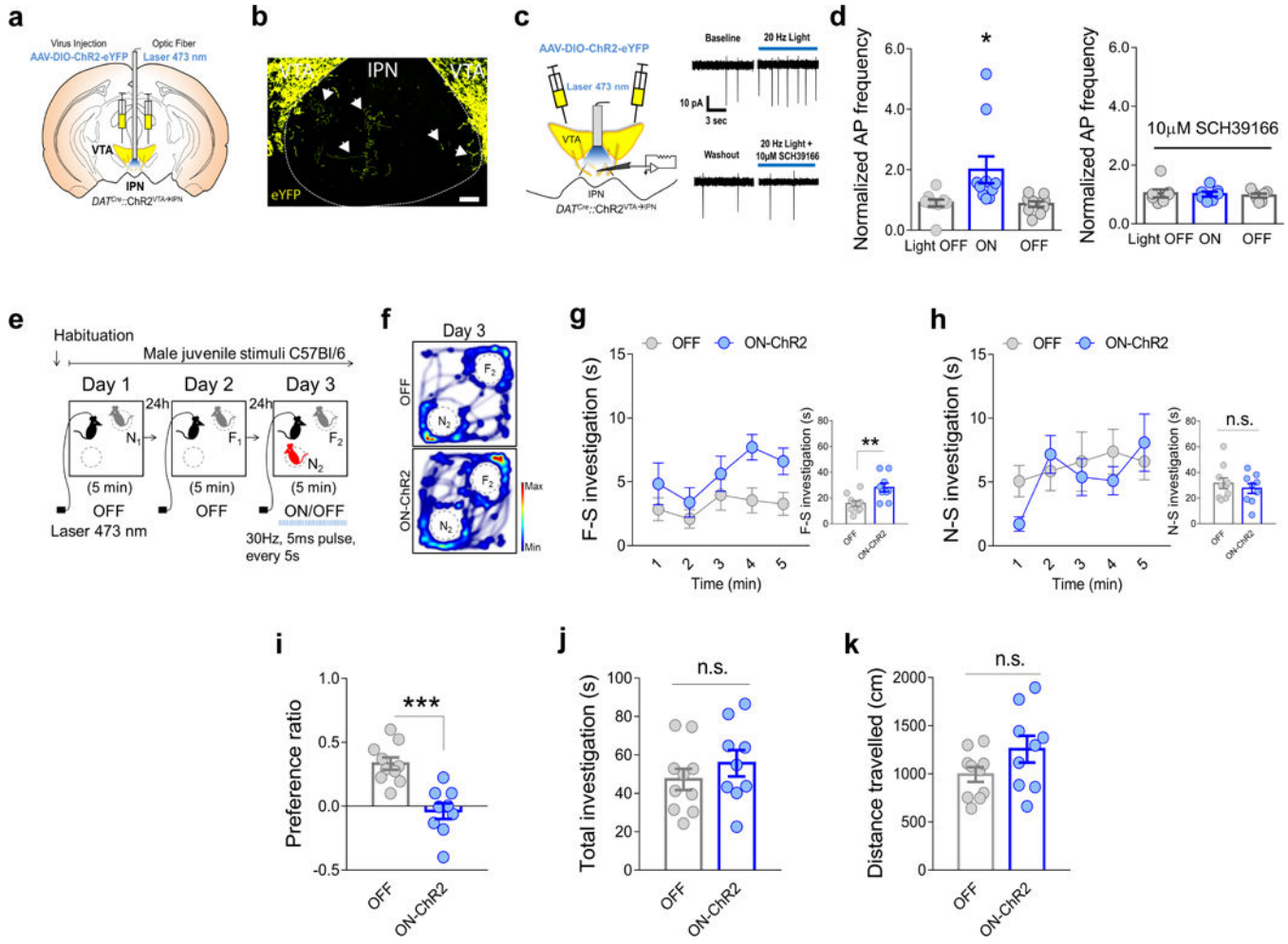

Figure 4. VTA sends functional DAergic input to the IPN to control social NP

(**a**) Schematic of viral injections in the VTA and optic stimulation strategy in the IPN of DAT^{Cre} mice. (**b**) Representative images of ChR2-eYFP expression in the VTA (yellow). Note axon projections to the IPN central and lateral regions (arrowheads). Scale bar 50 μm. (**c**) Left: experimental configuration for recordings to determine functional DAergic neuron VTA→IPN connection. Right: representative cell-attached AP recordings from caudal IPN neurons in midbrain slice from ChR2 VTA-infected DAT^{Cre} mice are shown at baseline, during $ChR2^{VTA→IPN}$ photo-stimulation (20 Hz) (top), and during photo-stimulation in the presence of the D1 antagonist SCH39166 (bottom). (**d**) Average normalized spontaneous AP frequency of caudal IPN neurons increased during photo-stimulation of VTA DAergic terminals (n = 10 neurons combined across 4 mice) (left, one-way RM ANOVA $F_{2,29} = 5.17$, *p = 0.0479), and was completely blocked by SCH39166 (n = 7 neurons combined across 4 mice) (right, one-way RM ANOVA $F_{2,20} = 0.68$, p = 0.4455). (**e**) Schematic of experimental approach used to measure interactions with F-S and N-S stimuli in DAT^{Cre}::$ChR2^{VTA→IPN}$ mice for the social NP task. (**f**) Representative heat maps showing the location of testing mice during the social NP task under light-OFF (top) (n = 10 mice) and light-ON conditions (bottom) (n = 9 mice). (**g**) Time of F-S investigation each minute of the social NP task increased upon VTA→IPN DAergic photo-stimulation. (Inset) Average total time of F-S

investigation (unpaired *t*-test, $t_{17} = 3.20$, **p = 0.0052). (**h**) Time of N-S investigation each minute of the social NP task. (Inset) Average total time of N-S investigation (unpaired *t*-test, $t_{17} = 0.71$, p = 0.4877). (**i**) Novelty preference ratio (unpaired *t*-test, $t_{17} = 4.81$, ***p = 0.0002). (**j**) Total investigation time (unpaired *t*-test, $t_{17} = 0.96$, p = 0.3492) and (**k**) travelled distance (unpaired *t*-test, $t_{17} = 1.71$, p = 0.1054). Data are expressed as mean ± s.e.m., n.s. not significant.

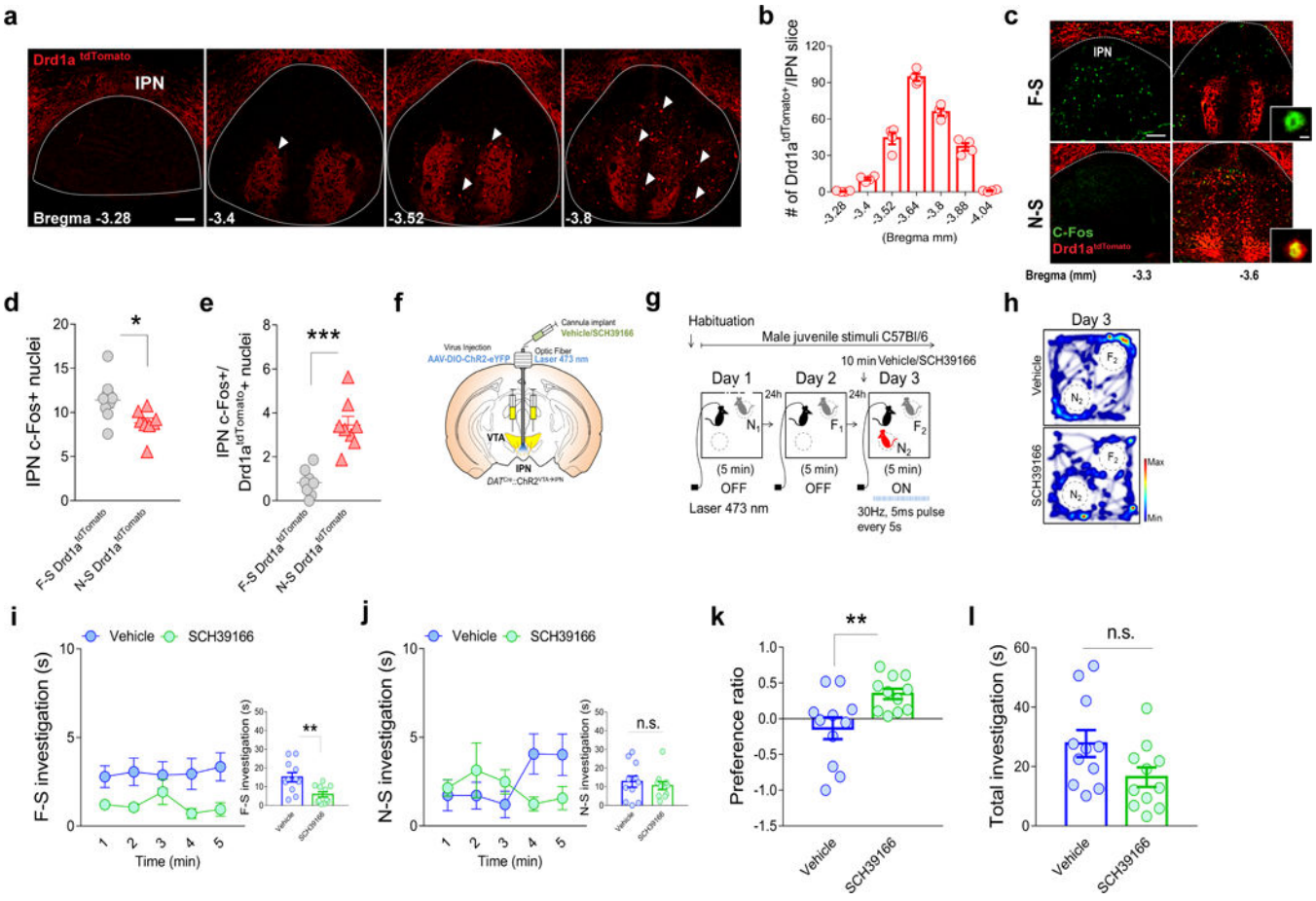

Figure 5. IPN D1 signaling drives DAergic VTA→IPN input that modulates social NP

(**a**) Representative images of D1 DsRed fluorescence at different IPN Bregma coordinates of *Drd1a*^{tdTomato} mice. Arrowheads show IPN D1^{+} cell bodies. Scale bar 50 μm. (**b**) Anatomical distribution of D1^{+} soma in the IPN (n = 4 mice). In *Drd1a*^{tdTomato} mice after F-S (n = 8 mice) or N-S (n = 8 mice) stimuli interactions: (**c**) Representative images of Fos immunoreactivity (green) and D1 DsRed fluorescence in the IPN. Note Fos colocalization with D1 expression (insets) occurs with N-S stimuli encounters. Scale bars (50 μm lower magnification; 20 μm higher magnification). (**d**) The total number of IPN Fos immunopositive nuclei was higher in the F-S group (unpaired *t*-test, $t_{14} = 2.48$, *p = 0.0262) but (**e**) the number of IPN Fos nuclei colocalized with D1 DsRed fluorescence was increased in the N-S group (unpaired *t*-test, $t_{14} = 5.78$, ***p < 0.0001). (**f**) Schematic of optogenetic injections in the VTA and optic stimulation plus drug infusion strategy in IPN of DAT^{Cre} mice. (**g**) Schematic of experimental approach used for interactions with F-S and N-S stimuli. On day 3 vehicle or D1 antagonist (SCH39166) were infused into the IPN prior to ChR2 stimulation. For DAT^{Cre}::ChR2$^{VTA→IPN}$ mice (all receiving light photo-stimulation): (**h**) representative heat maps showing the location of testing mice during the social NP task for vehicle- (top,n = 11 mice) or SCH39166-infused mice (bottom,n = 11 mice). (**i**) Time of F-S investigation each minute of the social NP task. (Inset) Average total time of F-S investigation (unpaired *t*-test, $t_{20} = 3.20$, **p = 0.0044). (**j**) Time of N-S investigation each minute of the social NP task. (Inset) Average total time of N-S investigation (unpaired *t*-test,

t_{20} = 0.58, p = 0.5660). (**k**) Preference ratio increased with SCH39166 infusion (unpaired *t*-test, t_{20} = 2.87, **p = 0.0096). (**l**) Total investigation time (unpaired *t*-test, t_{20}= 2.03, p = 0.0562). Data are expressed as mean ± s.e.m., n.s. not significant.